# Correlation functions of the hard-sphere Lorentz model

W. Götze and E. Leutheusser
*Max-Planck-Institut für Physik und Astrophysik, 8000 München, Germany*
*and Physik-Department der Technischen Universität München, 8046 Garching, Germany*

Sidney Yip
*Department of Nuclear Engineering, Massachusetts Institute of Technology, Cambridge, Massachusetts 02139*
(Received 12 March 1981)

Quantitative results for the correlation functions for the Lorentz model of overlapping hard spheres are worked out and discussed within the recently proposed theory of diffusion and localization of a classical particle moving in a random static field. The applicability of the theory to the diffusion phase is established by a successful comparison of the diffusivity as a function of density and the velocity-autocorrelation function as a function of time for various densities, with the computer simulation results of Bruin. Specific predictions of the localization length as a function of density, of a nonmonotonic density dependence of the effective power-law exponent of the long-time tail of the velocity correlations, and of an oscillatory wave-number dependence of the normalized width of van Hove's scattering function are presented.

## I. INTRODUCTION

The Lorentz model for the motion of a particle in an environment of randomly distributed hard-sphere scatterers exhibits a number of features relevant to the understanding of the diffusion dynamics in classical fluids.[1] Two theoretical features beyond the standard kinetic-equation results have been revealed by asymptotic expansions in the weak-coupling regime: The diffusivity is a nonanalytic function of the density[2] and the velocity spectrum is a nonanalytic function of frequency.[3] The velocity-autocorrelation function has also been calculated for small densities within the repeated ring collision approximation.[4] Computer simulation studies were carried out by Bruin[5,6] to obtain the diffusivity and the velocity-autocorrelation function for small and intermediate densities. The data indicate a percolation edge separating a phase with nonzero diffusivity from one where there is absence of diffusion. Computer simulations for the two-dimensional Lorentz model[7] detected the mentioned phase transition rather convincingly.

Recently an approximate theory for the evaluation of the correlation functions for the Lorentz model of overlapping hard-sphere scatterers has been proposed.[8] This theory reproduced the earlier theoretical results for the model[2,3] and yielded a phase transition at a critical concentration in agreement with the edge value which one can read off from Bruin's data.[5] In this paper, the computer data[5,6] are compared quantitatively with the results of the theory[8] and additional properties of the model are presented to challenge further simulation studies or possible neutron scattering experiments.

## II. THE MODEL

The model under consideration is specified by only one nontrivial parameter, the density of the scatterers $n$ measured relative to the volume of the spheres with radius $\sigma$,

$$n^* = n\sigma^3 . \tag{1a}$$

The constant particle velocity $v_0$ defines the frequency scale through the binary collision rate

$$\nu = \pi n^* v_0/\sigma , \tag{1b}$$

while the classical mean free path can be used as length scale

$$l = \sigma/\pi n^* . \tag{1c}$$

The central concept of the theory is the current relaxation kernel $M(z)$, a causal function of the complex frequency $z$. One gets $M(\omega \pm i0) = M'(\omega) \pm iM''(\omega)$ with $M''$ denoting the real, even, nonnegative absorptive part and $M'$ the reactive part. A Kramers-Kronig relation determines $M(z)$ as a spectral integral in terms of $M''(\omega)$. The kernel yields the correlation function of the velocities, the Laplace transform of $K(t) = \langle v(t)v \rangle$, as

$$K(z) = -\frac{1}{z + M(z)}(v_0^2/3) . \tag{2a}$$

The absorptive part of $K(z)$ determines the velocity-autocorrelation function as the Fourier transform

$$K(t) = \int_{-\infty}^{\infty} \cos\omega t \, K''(\omega) d(\omega/\pi) . \tag{2b}$$

$K(t)$ is of primary interest in any discussion of particle motion in disordered systems[9]; $K''(\omega)$ is

 

the analog of the real part of the electrical conductivity in the residual resistivity problem of metals or semiconductors. If the zero-frequency limit of $M$ exists, there is a nonzero dc conductivity implying a diffusivity

$$D=(v_0^2/3)1/M''(\omega),\quad \omega=0\ . \tag{3a}$$

If $M(z)$ exhibits a pole at zero frequency, then there is absence of diffusion. In this case particles move in a finite spatial region characterized by the localization length $l_0$,

$$l_0^2=-(v_0^2/3)/\omega M'(\omega),\quad \omega=0\ . \tag{3b}$$

The propagation of the particle is described most conveniently by van Hove's incoherent scattering function[9]

$$S(q,\omega)=\int_{-\infty}^{\infty}\cos\omega t\langle\exp\{i\vec{q}[\vec{r}(t)-\vec{r}(0)]\}\rangle dt\ . \tag{4a}$$

This quantity is obtained from the spectral function of the density propagator

$$S(q,\omega)=\phi''(q,\omega)/\pi\ , \tag{4b}$$

where $\phi(q,z)$ is related to the current relaxation kernel $M(z)$.[8]

## III. THE APPROXIMATION SCHEME

The theory for the kernel $M(z)$ leads to a nonlinear equation[8]

$$M(z)=i\nu-\tfrac{8}{9}n^*M(z)\int_0^\infty d\kappa\sigma\,\frac{F\left[\kappa\sigma,\left(\frac{z+M(z)}{\kappa v_0}\right)\right]^2}{1+M(z)\phi^{(0)}(\kappa,z+M(z))}\ . \tag{5}$$

In this equation enters the density-correlation function for the free particle

$$\phi^{(0)}(q,z)=\frac{1}{(qv_0)}\,\phi_0(z/qv_0)\ , \tag{6a}$$

where

$$\phi_0(x)=\tfrac{1}{2}\log\frac{x-1}{x+1}\ , \tag{6b}$$

and the vertex $F$ is given in terms of spherical Bessel functions derivatives and free system correlations similar to $\phi_0$,

$$F(\kappa,x)=j_0'(\kappa)\phi_0(x)-i\tfrac{9}{4}j_1'(\kappa)\phi_1(x)-2j_2'(\kappa)\phi_2(x)+\cdots\ , \tag{6c}$$

$$\phi_1=1+x\phi_0\ , \tag{6d}$$

$$\phi_2=(3x\phi_1-\phi_0)/2\ . \tag{6e}$$

It is clear from Eq. (5) that the current relaxation rate $M''(\omega)$ has to be calculated self-consistently with the particle propagation. In addition to the binary collision rate $\nu$, there is a higher-order in the density contribution which is quite different depending on whether the particles move almost freely, or diffuse slowly, or oscillate in a trap. The latter is calculated by a mode-coupling approximation describing the decay of the particle momentum into pair excitations consisting of random potential fluctuations of momentum $\vec{\kappa}$ and particle modes. For the particle modes it was necessary to express the propagators for density, current, stress, etc., in terms of the corresponding functions for the free system and the kernel $M(z)$ by means of a generalized collision rate approximation. In this way one gets, e.g.,

$$\phi(q,z)=\frac{\phi^{(0)}(q,z+M(z))}{1+M(z)\phi^{(0)}(q,z+M(z))}\ . \tag{7}$$

For an analytical discussion of Eq. (5) the reader is referred to our preceding publication.[8] Outside the regime of small $n^*$, large $n^*$, and $n^*$ close to the critical point,

$$n_c^*=9/4\pi\ , \tag{8}$$

the solution for $M(z)$ has to be obtained by solving the transcendental equation [Eq. (5)] numerically. We have done this by a straightforward iteration. The procedure was started at large values of frequency $z$, since all functions there are close to the ones obtained from the kinetic-equation approach.

To understand the solution of the approximate equation outside the asymptotic regimes discussed before,[8] let us consider the $z=0$ limit. If there is diffusion one can introduce the dimensionless relaxation rate $\alpha=M''(\omega=0)/\nu>0$ and rewrite the self-consistency equation in the form $\alpha=f_D(\alpha)$ [compare Eq. (29) of Ref. 8]. Hence, $\alpha$ can be obtained as the intersect of the $f_D(\alpha)$ versus $\alpha$ curve with the diagonal [Fig. 1(a)]. $f_D(\alpha)$ starts off from unity for $\alpha=0$ and increases with increasing $\alpha$. The increase is larger if $n^*$ becomes bigger, since multiple-scattering events enhance the current relaxation rate. For large $\alpha$ one gets (Ref. 8) $f_D(\alpha)=\alpha(n^*/n_c^*)+O(1/\alpha)$. Hence, diffusive particle propagation is possible for $n^*<n_c^*$, and for $n^*>n_c^*$ there is absence of diffusion. For $n^*>n_c^*$ the self-consistent current relaxation concept does not allow for a zero-frequency velocity spectrum. If there is localization one can introduce the dimensionless inverse localization length squared $\alpha=(4l/l_0)^2$ and rewrite Eq. (5) in the form $\alpha=f_L(\alpha)$ [compare Eqs. (33) of Ref. 8]. The solution $\alpha$ again is obtained as the intersection of the diagonal with $f_L(\alpha)$; In Fig. 1(b), $f_L(\alpha)$ starts off linearly for large localization lengths, $f_L(\alpha)=\alpha(n^*/n_c^*)+O(\alpha^2)$ and it approaches (Ref. 8) $8/3\sqrt{\alpha}$ for large $\alpha$. Hence there is localization for $n^*>n_c^*$ and for very dense systems the localization length is proportional to the mean free path ob-

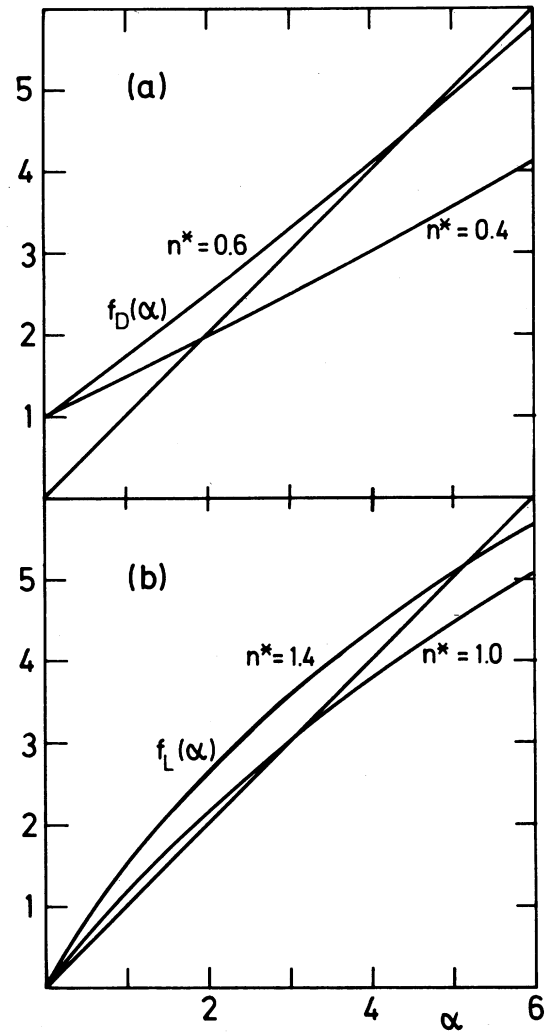


FIG. 1. Graphical solution of the self-consistency equations for (a) the diffusion phase $\alpha = D^{(0)}/D$ and (b) the localization phase $\alpha = (4l/l_0)^2$ (see text).

tained from the binary collision cross section $l_0 = l \cdot 3/2$. With decreasing density $l_0$ increases above $l$ until it diverges at the edge. For $n^* < n_c^*$ the self-consistency equations do not allow for a solution with localization.

## IV. RESULTS

In Figs. 2 and 3 the diffusivity as a function of $n^*$ is compared with the data of Bruin.[5,6] For $n^* < 0.2$ the agreement between theory and experiment is perfect, reflecting the fact that the theory reproduces correctly the leading correction to $D/D^{(0)} - 1 \propto n^*$ ($D^{(0)} = v_0^2/3\nu$). Notice that the non-regular $n^{*2}\log n^*$ term is so small that it does not show up in the figures. If one interpolates the experimental points by a linear $D/D^{(0)}$ vs $n^*$ function (dashed curves in Figs. 2 and 3) one obtains the percolation edge $n_c^*$ also in agreement with the present theory. For the sake of completeness in Fig. 2, the data for $n^* = 0.6$, and 0.8 are shown,[6] even though Bruin realized their uncertainties to be larger than for the other data. The source of greater uncertainty in the simulation data upon approaching $n_c^*$ will be discussed below in connection with Fig. 8. For intermediate densities the theory yields slightly greater diffusivities than the experiment.

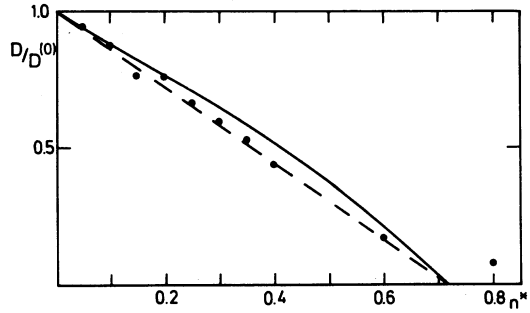


FIG. 2. Diffusivity $D$ normalized by the kinetic-equation result $D^{(0)}$ as function of density $n^*$. Dots are the simulation data of Bruin (Refs. 5 and 6). The full curve is the present theory. The dashed line is the linear function $(n_c^* - n^*)/n_c^*$.

The result the present theory predicts for the localization length $l_0$ is shown in Fig. 4. For $n^* > 2n_c^*$ $l_0$ is practically given by the large-coupling asymptote (dashed line in Fig. 4); near the edge $l_0$ diverges like $1/(n^* - n_c^*)^{1/2}$. A computer simulation of the dynamics would yield $l_0$ as the long-time mean spread $\langle \Delta x(t)^2 \rangle \to 2l_0^2$. The localization length determines the static polarizability as $\chi^0 = l_0^2$ and so a Monte Carlo computation would yield

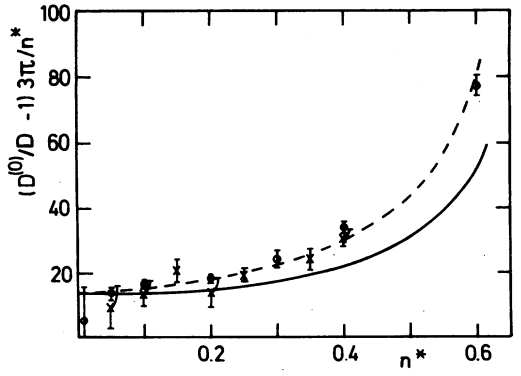


FIG. 3. Relative difference of the diffusivity $D$ to the kinetic-equation result $D^{(0)}$ as function of density $n^*$. Data and error bars are Bruin's results (Refs. 5 and 6), the full curve is the present theory, and the dashed line is the interpolation curve defined in Fig. 2.

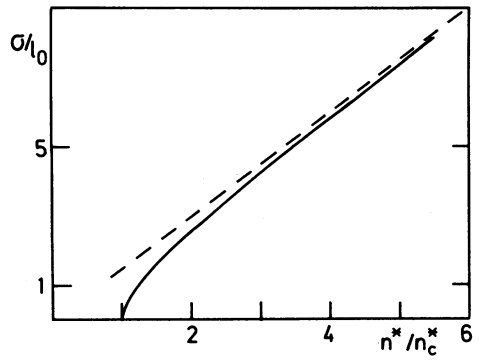


FIG. 4. Inverse localization length $l_0$ as a function of density. The dashed line is the large $n^*$ asymptote (Ref. 8).

$l_0^2$ as the dipole moment per field induced by a small homogeneous external field. Computer simulations for $l_0$ or $\chi^0$ or any other quantity for $n^* > n_c^*$ will be time consuming. The system is in a nonergodic phase then and so statistical fluctuations will be large.

For the weak-coupling system the velocity-correlation function is the classical exponential $K^{(0)}(t) = \exp(-\nu t)(v_0^2/3)$. With increasing density diffusivity is suppressed, hence $K(t)$ falls below $K^{(0)}(t)$. If the correlation effects become sufficiently pronounced, they give rise to a "backscattering" effect. In good agreement with the data of Bruin[5,6] the theory yields $K(t) < 0$ for $\nu t \gtrsim 2$ (Fig. 5). With increasing $n^*$, backscattering begins at earlier times (in units of $\nu^{-1}$), in correspondence with the decrease of $D/D^{(0)}$. For $n^* > n_c^*$, the positive area under the $K(t)$ curve exactly cancels the area of the part with backscattering. If $n^*$ increases, the magnitude of the negative part at intermediate times increases also somewhat at the expense of the tail for very long times. If one magnifies the scale of Fig. 5 by plotting $\Delta K(t) = K^{(0)}(t) - K(t)$, one realizes that the present theory underestimates a bit the magnitude of the negative tail of $K(t)$ for $\nu t > 2$ (Fig. 6).

The spectrum of the velocity-autocorrelation function $K''(\omega)$ (Fig. 7) also reflects the importance of the feedback mechansim underlying the present theory. According to the kinetic equation, $K^{(0)''}(\omega)\nu$ is a Lorentzian function of $\omega/\nu$ (dashed curve in Fig. 7). However, because $K''(\omega = 0) = D < D^{(0)}$, the correlation effects suppress the spectrum for small frequencies. For $\omega \gg \nu$, $K^{(0)''}(\omega) \cong K''(\omega)$, and since the area under the $K''(\omega)$ curve is independent of the interaction, $K''(\omega)$ has to exceed $K^{(0)''}(\omega)$ for intermediate frequencies $\omega$. For $n^* > n_c^*$, therefore, the spectrum has to exhibit a peak at some nonzero value of $\omega$, and by continuity there is such a peak also for intermediate $n^* < n_c^*$. The spectrum looks similar to that of a strongly damped oscillator. For intermediate frequencies there is no remarkable difference between the spectrum for the system below and above the percolation edge. The low-frequency variation of $K''(\omega)$ is quite different for the various density regimes.[8] For $n^* < n_c^*$ the spectrum

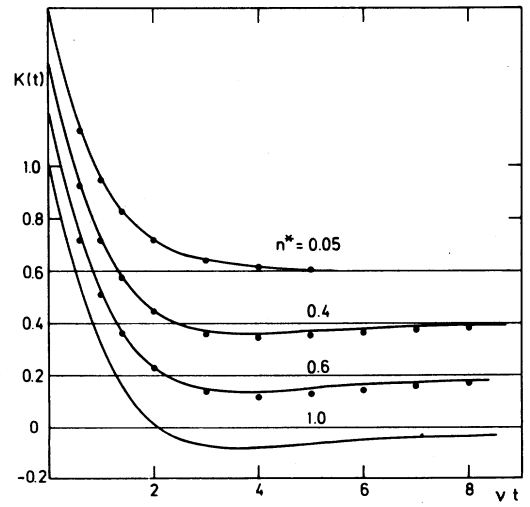


FIG. 5. Velocity-autocorrelation function $K(t)$ in units of $(v_0^2/3)$ as a function of time for various densities $n^*$. Dots are computer simulation results of Bruin (Refs. 5 and 6). The curves are the results of the present theory.

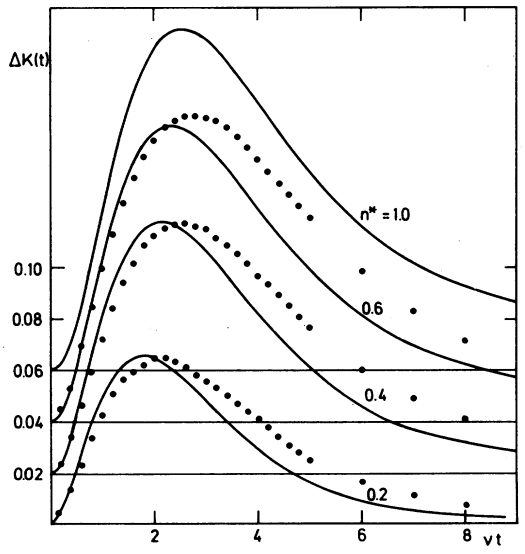


FIG. 6. Deviation of the velocity-correlation function from the kinetic theory result in units of $(v_0^2/3)$ as function of time for various densities. Dots are the Bruin data (Refs. 5 and 6). The curves are the results of the present theory.

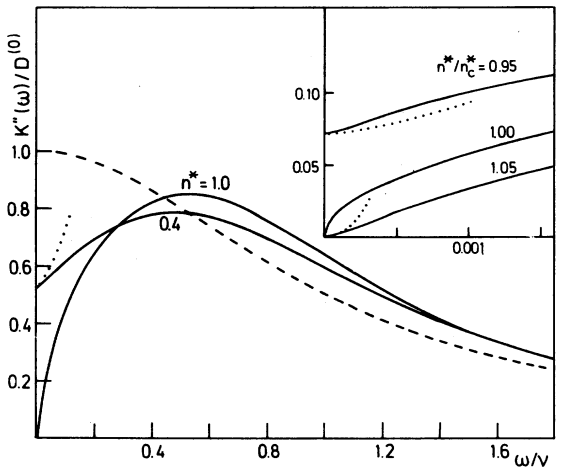


FIG. 7. Velocity spectrum $K''(\omega)$ as a function of frequency for various densities according to the present theory (full curves). The dashed curve is the kinetic-equation result $K^{(0)''}(\omega)$. The dotted curves are the low-frequency asymptotes (Ref. 8).

increases proportionally[3] to $\omega^{3/2}$, for $n^*=n_c^*$, $K'' \propto \omega^{1/2}$, and for $n^*>n_c^*$, $K'' \propto \omega^2$. Notice that the frequency scale has to be expanded considerably in order to make these different frequency variations visible.

An important consequence of the anomalous frequency spectrum $K''(\omega)$ is the shrinking of the hydrodynamic regime upon approaching the edge.[8] Let us define a characteristic frequency $\omega_h$, or time $t_h=1/\omega_h$, delineating the regime of hydrodynamic motion by requiring $K''(\omega)/K''(0)$ for $n^*<n_c^*$ [or $K'(\omega)/K'(0)$ for $n^*>n_c^*$] to deviate from a constant by not more than 5%. Diffusion and its associated $t^{-5/2}$ long-time tail can be observed only for $t>t_h$. Similarly, for $n^*>n_c^*$ $\langle \Delta x(t)^2 \rangle$ approaches its constant long-time value $2l_0^2$ only for $t>t_h$. In the classical weak-coupling regime one expects the hydrodynamic regime to expand with increasing coupling $t_h \sim 1/\nu$; the present theory verifies this result up to about $n^* \sim 0.5 n_c^*$, (Fig. 8). The same behavior is predicted for $n^*>2n_c^*$. At the edge there is no hydrodynamic motion and so it is evident that $t_h$ diverges if $n^* \to n_c^*$. The scaling law derived for $K''(\omega)$[8] reveals $t_h \propto 1/(n^*-n_c^*)^2$ near the edge. One has to wait longer the closer $n^*$ is to $n_c^*$ in order to decide, e.g., whether $\langle \Delta x(t)^2 \rangle / t$ approaches a constant as is to be expected for $n^*<n_c^*$, or whether $\langle \Delta x(t)^2 \rangle$ tends to $2l_0^2$ as one expects for $n^*>n_c^*$. Figure 8 represents $t_h$ as a function of $n^*$. For a computer experiment the maximal time $t_M$ is restricted by technical difficulties and therefore results for $D$ or $l_0$ can be obtained only for such densities with $t_h<t_M$. These physical circumstances are the reason why Bruin rightly suspected large uncertainties in his diffusivity results for $n^*=0.6$ and 0.8 (see Fig. 2). In principle there is a similar characteristic length scale $l_h$ diverging at $n_c^*$.[8] We found it not to be critical for the sample sizes used by Bruin[5,6] and therefore we do not show the corresponding graph.

The $\omega^{1/2}$ singularity of $K''(\omega)$ for $n^*=n_c^*$ implies a $t^{-3/2}$ long-time tail of $K(t)$. On the other hand one gets for $n^*<n_c^*$ and $t>t_h$ a $t^{-5/2}$ tail due to the $\omega^{3/2}$ singularity of $K''(\omega)$ in the diffusion phase and an essentially exponential decay of $K(t)$ for $n^*>n_c^*$.[8] To analyze this qualitative transition of the long-time anomaly in a computer simulation one can choose a window on the time axis $(1/\nu<)t_1<t<t_2$ and fit the velocity-correlation function by a power law $K(t) \propto t^{-\beta}$.[7] The exponent $\beta$ will depend somewhat on the window chosen. With increasing density $\beta$ will show the following variation. If $t_2>t_h$, the long-time exponent is essentially the classical one.[3] If $t_2 \sim t_h$, it drops until it reaches the critical value $\frac{3}{2}$ in the neighborhood $n^* \sim n_c^*$ where $t_h>t_2$. In the localized phase $\beta$ increases with increasing $n^*$ without upper bound. The quantitative prediction of the $\beta$ variation for the three-dimensional Lorentz model shown in Fig. 9 is made for the window $t_1\nu=20$ and $t_2\nu=50$.

Spatial and time-dependent effects both appear in the van Hove self-correlation function, Eqs. 4(b) and (7). For the noninteracting systems $S^{(0)}(q,\omega)$ is the constant $1/(2qv_0)$ for frequencies

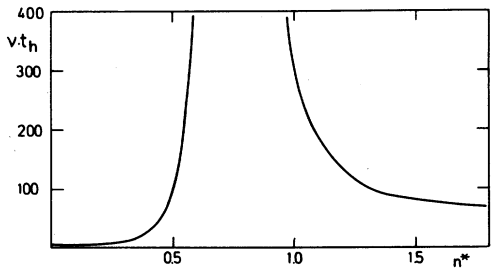


FIG. 8. Characteristic time scale $t_h$ delineating the regime for hydrodynamic motion.

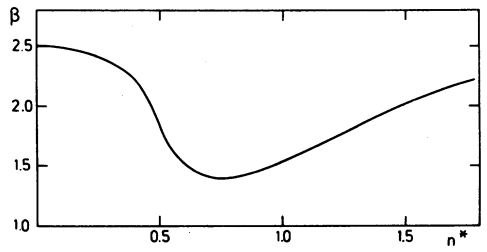


FIG. 9. Effective long-time exponent as a function of density defined for the time window $t_1\nu=20$, $t_2\nu=50$.

smaller than $qv_0$ and zero otherwise. Owing to the collisions, $S(q,\omega)$ is essentially bell shaped for small and intermediate values of $ql$ (Fig. 10). For $ql>10$ the recoil spectrum $S(q,\omega)$ essentially is the free function $S^0(q,\omega)$ with a small peak superimposed at $\omega\sim 0$. To make the anomaly of the dynamics transparent, one can characterize $S(q,\omega)$ by its half-width at half-maximum $\omega_{1/2}(q)$ and plot this quantity as a function of $q$ relative to the diffusion width $\gamma(q)=\omega_{1/2}(q)/D^{(0)}q^2$ (Ref. 10), see Fig. 11. $\gamma(q)$ can be looked upon as an effective diffusion constant. In the hydrodynamic regime, $\gamma(q)\simeq\gamma(q=0)=D/D^{(0)}$. If one evaluates $\phi(q,z)$ from the Boltzmann equation, the correlation function is given by Eq. (7) with $M(z)=i\nu$.[2,11] One finds $\gamma(q)$ to be unity for wave numbers smaller than the inverse mean free path $l$ and then it drops monotonically. In the kinetic-equation approximation, $\phi(q,z)$ approaches the free particle function for $ql>1$ with width $\omega_{1/2}(q)=qv_0$, dashed dotted curve in Fig. 11. For small densities, the present theory reveals for $\gamma(q)$ a similar behavior except for a decrease of $\gamma(q=0)$ due to suppression of the diffusivity; see the result for $n^*=0.2$ in Fig. 11. At intermediate densities, however, $\gamma(q)$ exhibits an oscillatory behavior. It decreases with increasing wave number to reach a broad minimum at about $ql\sim 1$, then it increases again to reach a maximum somewhat greater than $\gamma(q=0)$. For large $q$, $\gamma(q)$ decreases like the kinetic-equation result. The low-$q$ decrease of the effective diffusion constant can be understood by carrying out a long-wavelength expansion of the density-correlation function, Eq. (7). In leading nontrivial order of the small parameter $\{qv_0/[z+M(z)]\}^2$, one finds $\phi(q,z)$ to be a generalized diffusion propagator

$$\phi(q,z)=\frac{-1}{z+K(z)q^2}\,,\quad q\to 0 \tag{9a}$$

with the frequency-dependent diffusion constant $K(z)$. Expanding the denominator of Eq. (9a) for small $z=\omega+i0$ one finds

$$\phi(q,\omega+i0)=\frac{-1}{\omega+iD^{(0)}q^2\gamma(q)}\,\frac{\gamma(q)}{D/D^{(0)}}\,, \tag{9b}$$

with

$$\gamma(q)=\frac{D/D^{(0)}}{1+\left(\frac{\partial K'}{\partial\omega}(\omega=0)\right)q^2}\,. \tag{9c}$$

The strong suppression of the velocity spectrum at low frequencies as opposed to intermediate frequencies, (Fig. 7), implies $K(\omega)$ to exhibit normal dispersion for $\omega\sim 0$: $\partial K'/\partial\omega>0$. Hence, $\gamma(q)$ decreases with increasing $q$ as long as expansions (9) are applicable. If $ql\sim 1$, the frequency at half-width of $S(q,\omega)$ is of order $\nu$. Then $K(z)$ approaches the kinetic-equation result $M(z)\simeq i\nu$, see Fig. 7. As a result, $\phi(q,z)$ practically becomes the kinetic-equation result and this implies a corresponding increase of $\gamma(q)$ to the dashed-dotted line of Fig. 11. So according to the present theory the $\gamma(q)$ oscillation represents a percursor phenomenon for the phase transition to the localization regime. It should be mentioned that the $\gamma(q)$ oscillation has been observed for the incoherent scattering function in classical liquids by computer simulation[10,11] and by neutron scattering experiments,[13] and that the preceding interpretation is in agreement with the semiphenomenological theory[14] proposed to explain these data. Obviously it would be desirable to extend the existing computer simulations in order to check the quantitative predictions (Figs. 10 and 11) of the present work. Such a check would test essentially the

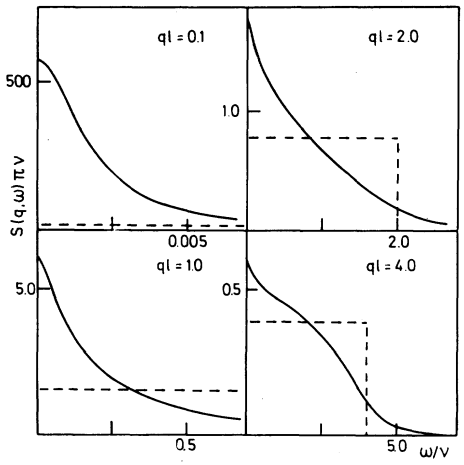


FIG. 10. Van Hove function $S(q,\omega)$ as a function of frequency $\omega$ for various wave numbers $q$; $n^*=0.4$. The dashed curves are the free-particle results $S^{(0)}(q,\omega)$.

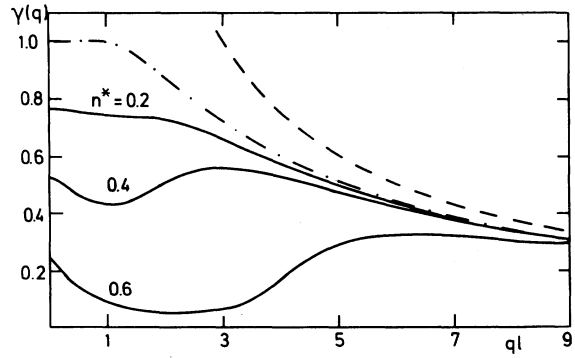


FIG. 11. Effective diffusion constant $\gamma(q)$ as function of the wave number $q$ for various densities. The dashed curve is the free-particle result $\gamma(q)\propto 1/(qv_0)$, the dashed-dotted curve is the result of the kinetic-equation approach.

quality of the approximation for $\phi(q,z)$, Eq. (7).[15]

It should be mentioned that all the graphs presented thus far have been evaluated taking into account the first three terms contributing to the vertex $F$ [Eq. (6c)]. To justify this procedure, the convergence is analyzed for the most sensitive function $\Delta K(t)$ discussed above in connection with Fig. 6. Taking into account only the density mode in Eq. (6c) corresponds to the approximation studied originally for the diffusion-localization phase transition.[15] This approximation accounts qualitatively for all the features of the preceding results and yields the correct value of the percolation density $n_c^*$. The leading approximation, however, does not reproduce correctly the prefactor of the long-time anomaly for small $n^*$, nor the correct singular low-density expansion of $D$. The latter defects are eliminated if the first two contributions to $F$ in Eq. (6c) are taken into account,[8] but convergence in the sum (6c) is not achieved if only $\phi_0$ and $\phi_1$ are considered. Figure 12 demonstrates that taking into account the first four terms in the series for $F$ (dotted line) does not significantly modify the three-mode result (full curve). The next correction beyond the four-mode approximation is so small, that the corresponding result for $\Delta K(t)$ cannot be distinguished from the dotted curve of Fig. 12.

If one is interested in the main qualitative features of the theory only, i.e., in a self-consistent and unified treatment of diffusion and localization, one can simplify the mathematics considerably as follows. First one restricts Eq. (6c) to the leading term so that Eqs. (7) and (5) yield

$$M(z)=i\nu+\tfrac{8}{9}n^* v_0^2\sigma \times\int_0^\infty d\kappa\,\kappa^2 j_1^2(\kappa\sigma)[\phi(\kappa,z)-\phi^{(0)}(\kappa,z+M(z))]. \tag{10a}$$

Second, one neglects $\phi^{(0)}$ in comparison to $\phi$ and replaces the latter by the long-wavelength asymptote, Eq. (9a). Then the momentum integral can be expressed in terms of Bessel functions with imaginary argument. With the abbreviation $K^{(0)}(z)$

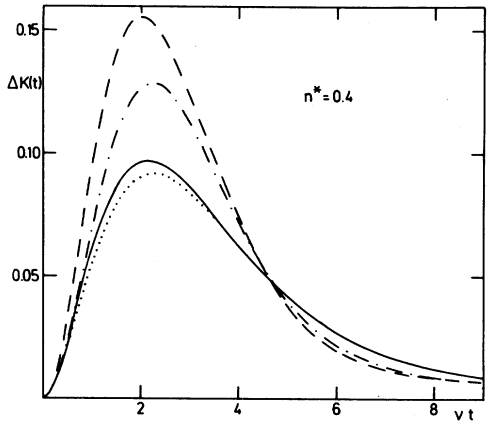


FIG. 12. Results for $\Delta K(t)$ compare Fig. 6 for various approximations of the vertex (see text). Dashed-dotted line: 0-contribution. Dashed line: 0-1 contribution. Full line 0-1-2 contribution. Dotted line: 0-1-2-3 contribution.

$=-(v_0^2/3)/(z+i\nu)$, the self-consistency equation reduces to the transcendental equation for $K(z)$,

$$\frac{K(z)}{K^{(0)}}(z)=1-\frac{n^*}{n_c^*}\,F([z\sigma^2/K(z)]^{1/2}), \tag{10b}$$

$$F(\xi)=3I_{3/2}(\xi)K_{3/2}(\xi). \tag{10c}$$

In particular, one gets for $z=0$ $D/D^{(0)}=1-n^*/n_c^*$, i.e., the dashed line in Fig. 2. The rather good result of this treatment for $D$ is accidental, however, the velocity-autocorrelation function derived from Eqs. (10) does not account adequately for Bruins $K(t)$ data.[5,6]

## ACKNOWLEDGMENTS

We would like to thank Dr. C. Bruin for sending us his computer simulation results and for permission to use unpublished data. One of us (S. Y.) expresses his appreciation to the Alexander-von-Humboldt-Foundation for a U. S. Senior Scientist Award and to the Physik-Department, Technische Universität München for hospitality. The work of S. Y. is supported in part by the National Science Foundation.

[1]For a general discussion see E. H. Hauge, in *Lecture Notes in Physics*, edited by G. Kirczenow and J. Marro (Springer, Berlin, 1974), Vol. 31, p. 337.

[2]J. M. J. van Leeuwen and A. Weyland, Physica (Utrecht) 36, 457 (1967); A. Weyland and J. M. J. van Leeuwen, *ibid.* 38, 35 (1968).

[3]M. H. Ernst and A. Weyland, Phys. Lett. 34A, 39 (1971).

[4]T. Keyes and J. Mercer, Physica (Utrecht) 95A, 473 (1979).

[5]C. Bruin, Phys. Rev. Lett. 29, 1670 (1972); Physica (Utrecht) 72, 261 (1974).

[6]C. Bruin, Ph.D. thesis, Delft University, 1978 (unpublished).

[7]B. J. Alder and W. E. Alley, J. Stat. Phys. 19, 341 (1978).

[8]W. Götze, E. Leutheusser, and S. Yip, Phys. Rev. A 23, 2634 (1981).

[9]P. A. Egelstaff, *An Introduction to the Liquid State* (Academic Press, London, 1967).
[10]B. R. A. Nijboer and A. Rahman, Physica (Utrecht) 32, 415 (1966).
[11]M. Nelkin and A. Ghatak, Phys. Rev. 135A, 4 (1964); S. Ranganathan and S. Yip, Physica (Utrecht) 100A, 127 (1980).
[12]D. Levesque and L. Verlet, Phys. Rev. A 2, 2514 (1970).
[13]K. Sköld, J. M. Rowe, G. Ostrowsky, and P. D. Randolph, Phys. Rev. A 6, 1107 (1972).
[14]W. Götze and A. Zippelius, Phys. Rev. A 14, 1842 (1976).
[15]W. Götze, Solid State Commun. 27, 1393 (1978); J. Phys. C 12, 1279 (1979); Philos. Mag. B43, 219 (1981).